

Propagation of fluid-loaded structural waves along an elastic duct with smoothly-varying bending characteristics

by

A. D. Grant and J. B. Lawrie

Department of Mathematical Sciences

Brunel University, Uxbridge, Middlesex, UB8 3PH.

jane.lawrie@brunel.ac.uk

Abstract

This article is concerned with the sound field generated by a fluid-loaded structural wave travelling along the boundary of a two-dimensional duct with walls that have smoothly varying elastic properties. It is the field within the duct that is of interest and the exterior region is assumed to be in vacuo. By recourse to a modified form of the two-dimensional plate equation the boundary-value problem is posed in terms of the fluid velocity potential. A functional difference equation method is used to obtain an explicit integral solution from which the reflection and transmission coefficients are determined. Various limiting forms of the modified plate equation are discussed together with the implications each has on both the analytic method used herein and the physical situation it describes.

1 Introduction

Acoustic scattering by structures that have abrupt changes in either geometry or material properties pose many technical problems for scientists and engineers. For example welds, rivets and small physical variations in the properties of adjacent panels in an aircraft wing all give rise to scattering of fluid-coupled structural waves. It is essential for design engineers to understand the qualitative effects of, for example, sudden variation in panel depth or the presence of a weld. Presence of two or more such features gives rise to the possibility of resonance, which in turn could lead to structural fatigue. For these reasons scattering by a wide variety of key structural features has been studied extensively. Problems involving structures that have planar boundaries with abrupt change in material properties may be amenable to solution by the Wiener-Hopf technique. Recent work on examples of this type include Brazier-Smith [3], Norris and Wickham [11] and Cannell [4, 5]. For nonplanar boundaries, there are no standard solution methods. Structures comprising two planar surfaces that are joined together to form a wedge may be solved by recourse to the Kontorovich-Lebedev transform [1, 14], or the Sommerfeld integral [2, 13]. Other geometric discontinuities that are amenable to analytic solution include problems involving wave propagation in a duct with abrupt change in height [17]. Scattering by structures in which the material properties vary smoothly in space as opposed to discontinuously have, for a variety of reasons, received little attention, although a finite transition region may be a better model of many real materials. Work by Roseau [15], Evans [7], and Evans and Fernyhough [8] applies one of the few mathematical techniques available for this kind of problem. Roseau solved a water-wave problem where the depth of water varied owing to a sloping bottom with a continuous, nonlinear profile. By representing the fluid velocity potential as a Fourier integral Roseau was able to recast the boundary-value problem as a functional difference equation of a well-known class. Evans was able to employ the same

technique to solve another water-wave problem in which particles of varying density float on the surface of a body of water of constant depth. Evans and Fernyhough then extended the method to deal with the problem of scattering in an acoustic waveguide in which the bounding surface had smoothly varying impedance.

This article deals with acoustic scattering by a duct in which one wall comprises an elastic plate with properties varying continuously in one space direction. Specific details as to which parameters vary are left until later in the text; however, a simple example is smooth variation in plate thickness. The model is intended as a heuristic investigation of this class of problem. The physical parameters are assumed to vary according to a simple heuristic mathematical law [15, 7]. The aim is to understand qualitatively the effects of a smooth change in material properties rather than quantify a specific physical situation.

In section 2 the equation governing small lateral vibrations of a thin, loaded plate with nonuniform properties is derived for the case of cylindrical bending. It is assumed that one or more of Young's modulus, Poisson ratio and area density vary across the plate in one direction. In section 3 the model boundary-value problem is set up using the Helmholtz equation and a modified form of the plate equation of section 2. Exact solution to the boundary-value problem is obtained in section 4 by recourse to the difference-equation method. In section 5 expressions are obtained for the principal reflected and transmitted modes in the duct resulting from an incident wave. The discussion in section 6 considers limiting cases in which the variation in material properties is either particularly abrupt or extremely gradual. Comparisons with the Wiener-Hopf analogy are drawn and the implications for future work are discussed.

2 The plate equation

Before formulating the boundary-value problem that describes the sound field within the duct it is necessary to derive the equation governing vibrations of a loaded plate with non-uniform elastic properties. The following is based on the theory in [16], where different notation is used.

Figure 1 shows a rectangular portion of a thin elastic plate which is subjected to pressure causing slight cylindrical bending; the broken lines indicate a strip of the plate with unit width in the z -direction. In any thin, narrow layer of the

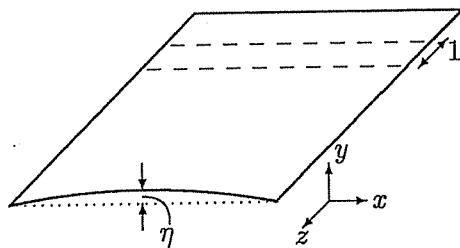


Figure 1: Rectangular portion of bent plate, showing the strip of unit width.

strip, located at a distance y from the neutral surface (see Figure 2 and the text below), the normal component of stress in the longitudinal direction of the layer, σ_x , can be expressed in terms of the Young's modulus $E(x)$, Poisson's ratio $\nu(x)$ and curvature, all of which are assumed to vary with x , as explained in the next paragraph.

The deflection of the plate is denoted by η and is taken as positive in the direction of increasing y . The curvature of the plate, regarded as positive when convex downwards, is approximated by $d^2\eta/dx^2$ so that the elongation in the x -direction of the layer under consideration is

$$\epsilon_x = -y \frac{d^2\eta}{dx^2}. \quad (1)$$

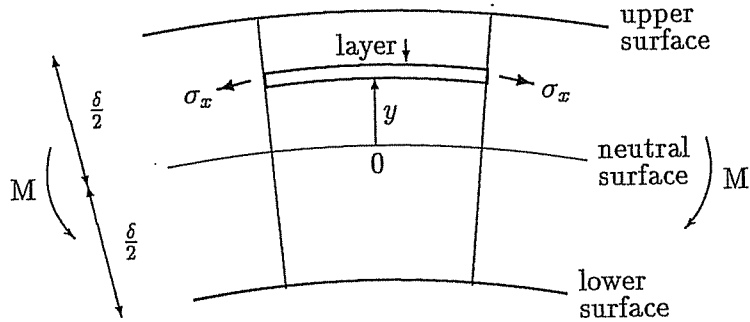


Figure 2: Section of strip, showing neutral surface and thin layer.

Hooke's law relates the normal stresses σ_x and σ_z to the unit elongations ϵ_x and ϵ_z by

$$\epsilon_x = \frac{\sigma_x}{E(x)} - \frac{\nu(x)\sigma_z}{E(x)}, \quad \epsilon_z = \frac{\sigma_z}{E(x)} - \frac{\nu(x)\sigma_x}{E(x)} = 0.$$

In the second of these equations the lateral strain ϵ_z must be zero to preserve the cylindrical shape, so that

$$\epsilon_x = \frac{1 - \nu(x)^2}{E(x)} \sigma_x,$$

and it follows from (1) that, for small deflections of the plate,

$$\sigma_x = -\frac{E(x)y}{1 - \nu(x)^2} \frac{d^2\eta}{dx^2}. \quad (2)$$

It should be noted that for the purposes of this section, y is measured from the neutral surface, that is the plane which is subject to neither compression nor tension during deformation. The curvature of the plate as drawn in Figure 2 is negative; for $y > 0$ the stress on the indicated layer is positive, causing elongation. (In following sections of this chapter the dimensional co-ordinate \hat{y} and its non-dimensional counterpart y are measured from the lower surface of the duct.) Equation (2) is an expression for the normal component of stress in the longitudinal direction in the case of varying Young's modulus (E) and Poisson ratio (ν). The reader is referred to [16] for further details.

The relation (2) is multiplied by y and integrated with respect to y through the thickness of the plate to give the equation of the deflection curve of the elemental strip, namely

$$B(x) \frac{d^2 \eta}{dx^2} = -M(x), \quad (3)$$

where

$$B(x) = \frac{E(x) \delta^3}{12 \{1 - \nu(x)^2\}}$$

is the bending stiffness (flexural rigidity) of the plate material and $M(x)$ the bending moment per unit distance in the x -direction. With reference to Figure 2, positive M is in the sense depicted, causing tension in the upper surface of the plate and compression in the lower.

If the plate is subjected to a loading $q(x)$ acting from below, the equation of equilibrium in terms of $M(x)$ is

$$\frac{d^2 M}{dx^2} = -q(x). \quad (4)$$

Provided that variable bending stiffness $B(x)$ is twice differentiable then, using (3) together with (4) the equation of equilibrium in terms of the lateral displacement is

$$B(x) \frac{d^4 \eta}{dx^4} + 2B'(x) \frac{d^3 \eta}{dx^3} + B''(x) \frac{d^2 \eta}{dx^2} = q(x). \quad (5)$$

This relates to cylindrical bending with varying bending stiffness. Further details can be found in [16]. In this chapter, the variation in the bending stiffness $B(x)$ is attributable to non-uniformity of Young's modulus, Poisson ratio and/or the area density of the plate, whereas Timoshenko and Woinowsky-Krieger envisage a plate with uniform material properties but varying thickness when deriving their equation. Whilst the varying thickness model may be the most obviously practical one, it is interesting to observe that the mathematical analysis is equally applicable to a plate of constant thickness but varying material, such as an alloy

containing changing proportions of metals, and to situations where both thickness and material vary in a suitable way.

Now consider a vibrating plate subject to fluid pressure $q(x, t)$ and with displacement $\eta(x, t)$. The equation governing lateral vibrations follows from (5) as

$$\frac{\partial^4 \eta}{\partial x^4} + \frac{2B'(x)}{B(x)} \frac{\partial^3 \eta}{\partial x^3} + \frac{B''(x)}{B(x)} \frac{\partial^2 \eta}{\partial x^2} = -\frac{m(x)}{B(x)} \frac{\partial^2 \eta}{\partial t^2} - [p]_{-}^{+}, \quad (6)$$

where $m(x)$ is the mass per unit area and $[p]_{-}^{+}$ the fluid pressure difference across the plate. In the case of motion with harmonic time dependence of angular frequency ω , this becomes

$$\frac{\partial^4 \eta}{\partial x^4} + \frac{2B'(x)}{B(x)} \frac{\partial^3 \eta}{\partial x^3} + \frac{B''(x)}{B(x)} \frac{\partial^2 \eta}{\partial x^2} - \frac{\omega^2 m(x)}{B(x)} \eta = -[p]_{-}^{+}. \quad (7)$$

The second and third terms of (7) vanish when the bending stiffness B is constant. It is thus to be expected that their effect on the mathematical analysis will be greater if $B(x)$ changes rapidly with x .

3 The boundary value problem

The boundary-value problem describes a two-dimensional infinite duct occupying the region $0 \leq \hat{y} \leq \hat{h}$ of a Cartesian coordinate system $(\hat{x}, \hat{y}, \hat{z})$ (see Figure 3). Note that, unlike § 2, dimensional quantities are here and henceforth indicated by a caret $\hat{\cdot}$. The lower duct wall, that is at $\hat{y} = 0$, is rigid whilst the upper wall comprises an elastic plate whose material properties vary continuously and monotonically between limiting values which are approached as \hat{x} becomes large in absolute value. A compressible fluid of mean density ρ_0 and sound speed c occupies the interior of the duct whilst the exterior region is *in vacuo*. The dimensional boundary-value-problem is formulated using (7) as the plate equation. This is non-dimensionalised with respect to length and time scales k^{-1} and

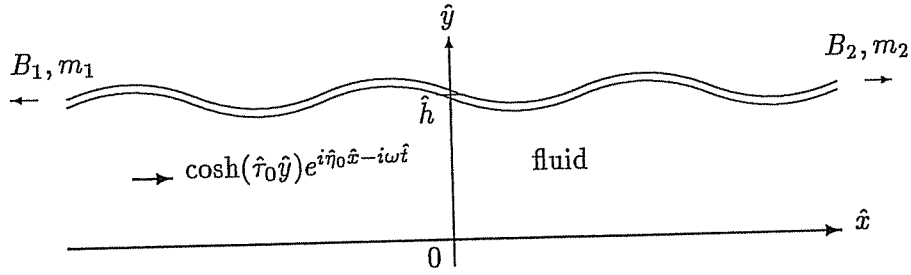


Figure 3: *The duct*

ω^{-1} and then modified to represent the situation in which the plate properties vary *slowly* with distance along the plate. The analysis is also applicable to the problem obtained by reflecting the configuration in the plane $\hat{y} = 0$ and removing the rigid surface there. (That is a 2-dimensional duct in which both boundaries comprise elastic plates.)

A fluid-coupled structural wave propagates along the elastic plate and is scattered due to the variation in the plate properties. The incident forcing has the form

$$\phi_0(\hat{x}, \hat{y}, \hat{t}) = A \cosh(\hat{\tau}_0 \hat{y}) e^{i \hat{\eta}_0 \hat{x} - i \omega \hat{t}}$$

where the wavenumbers $\hat{\eta}_0$ and $\hat{\tau}_0$ – or rather their non-dimensional equivalents – are defined later in the text. This incident wave has harmonic time dependence, of angular frequency ω . Both the incident wave and the elastic properties of the plate are independent of \hat{z} and thus fluid velocity potential may be written as $\Phi(\hat{x}, \hat{y}, \hat{t})$. The fluid pressure and plate elevation $\hat{\eta}$ are related to the velocity potential by

$$p(\hat{x}, \hat{y}, \hat{t}) = -\rho_0 \frac{\partial \Phi}{\partial \hat{t}}(\hat{x}, \hat{y}, \hat{t}), \quad \frac{\partial \hat{\eta}}{\partial \hat{t}} = \frac{\partial \Phi}{\partial \hat{y}}.$$

A steady state solution is sought and thus the acoustic field may be expressed as

$$\Phi(\hat{x}, \hat{y}, \hat{t}) = \Re\{\hat{\phi}(\hat{x}, \hat{y}) e^{-i \omega \hat{t}}\}.$$

For convenience, the harmonic time factor is henceforth suppressed.

CHAPTER 4. SMOOTHLY-VARYING BENDING

The steady state, time-independent potential $\hat{\phi}(\hat{x}, \hat{y})$ satisfies the Helmholtz equation

$$\left(\frac{\partial^2}{\partial \hat{x}^2} + \frac{\partial^2}{\partial \hat{y}^2} + k^2 \right) \hat{\phi} = 0; \quad \Re(k) > 0, \quad \Im(k) \geq 0, \quad (8)$$

where $k = \omega/c$ is the acoustic wavenumber. Although k is a real quantity, it is mathematically convenient to allow it to be complex with a small positive imaginary part. Physically this corresponds to a small dissipation of wave energy with distance. The lower bounding surface is described by the boundary condition

$$\hat{\phi}_{\hat{y}}(\hat{x}, 0) = 0,$$

and the upper one by (4.7) which, expressed in terms of $\hat{\phi}(\hat{x}, \hat{y})$, is

$$\left\{ \frac{\partial^4}{\partial \hat{x}^4} + \frac{2B'(\hat{x})}{B(\hat{x})} \frac{\partial^3}{\partial \hat{x}^3} + \frac{B''(\hat{x})}{B(\hat{x})} \frac{\partial^2}{\partial \hat{x}^2} - \frac{m(\hat{x})\omega^2}{B(\hat{x})} \right\} \hat{\phi}_{\hat{y}}(\hat{x}, \hat{h}) = \frac{\rho_0\omega^2}{B(\hat{x})} \hat{\phi}(\hat{x}, \hat{h}) \quad (9)$$

where ρ_0 is the density of the fluid in the absence of disturbance, $m(\hat{x})$ is the mass per unit area of the plate material and $B(\hat{x})$ its bending stiffness. The bending stiffness and mass per unit area are taken, cf (3.7), to have the forms

$$B(\hat{x}) = \frac{B_1 + B_2 e^{\hat{x}/\hat{a}}}{1 + e^{\hat{x}/\hat{a}}}, \quad m(\hat{x}) = \frac{m_1 + m_2 e^{\hat{x}/\hat{a}}}{1 + e^{\hat{x}/\hat{a}}}, \quad (10)$$

where \hat{a} is a positive constant determining the maximum rate of change of the function (which occurs at $\hat{x} = 0$). In the case $\hat{a} \gg 1$ the first and second derivative of $B(\hat{x})$ are small compared to $B(\hat{x})$ itself and this corresponds to *slow* variation of the properties of the plate along its length. In such circumstances a good approximation to the plate equation is obtained by neglecting the second and third terms on the left-hand side. However, this approximation is more widely valid. The reader is referred to the definitions of μ_j and α_j given below equation (22). For $\mu_j, \alpha_j > 1$, $j = 1, 2$ it is found that the approximation is valid provided that $a \geq 1$; in fact, for some ranges of the parameters μ_j, α_j it is possible to take smaller values of a . This can be seen by looking at the maximum values of $|B'/B|$ and $|B''/B|$. For example, it is required that

$$\begin{aligned}\mu_j^4 &\gg \max \left| \frac{B'(x)}{B(x)} \right| \\ &= \frac{1}{2a} \left| \frac{B_2 - B_1}{B_1 + B_2} \right|\end{aligned}$$

from which it follows that

$$a \gg \frac{1}{2\mu_j^4} \left| \frac{B_2 - B_1}{B_1 + B_2} \right|,$$

and a similar expression is obtained for the term $|B''/B|$. This chapter is primarily concerned with the situation in which the second and third terms of the differential operator of (9) can be neglected. Note, however, that this approximation is never valid for $a = 0$.

The usual radiation condition holds. That is, with the exception of the incident mode, all disturbances travel out to infinity as though initiating from the point $\hat{x} = 0$. For the geometric constraint $h = \hat{h}k < \pi/2$ with $\alpha_j/\mu_j^4 < \tan(\hat{h}k)$ the fluid velocity potential thus assumes the form

$$\hat{\phi}(\hat{x}, \hat{y}) = \begin{cases} (Ae^{i\hat{\tau}_0\hat{x}} + R_0e^{-i\hat{\tau}_0\hat{x}}) \cosh(\hat{\tau}_0\hat{y}) & \text{as } \hat{x} \rightarrow -\infty, \\ T_0 \cosh(\hat{\lambda}_0\hat{y})e^{i\hat{\nu}_0\hat{x}} & \text{as } \hat{x} \rightarrow +\infty, \end{cases} \quad (11)$$

where R_0 (T_0) is the complex reflection (transmission) coefficient of the fundamental mode. The wavenumbers $\hat{\nu}_0$ and $\hat{\lambda}_0$ are associated with the limiting properties of the plate for large positive values of \hat{x} and are defined later in the text.

The boundary-value problem is now expressed in a non-dimensional form by using a length scale of k^{-1} and a time scale of ω^{-1} . Non-dimensional variables, functions, wavenumbers and plate properties are denoted by symbols without carets. For example, $\hat{x}k = x$, $\hat{t}\omega = t$ and $\hat{\phi}k^2/\omega = \phi$. The formulation (8)-(11) becomes

$$\left(\frac{\partial^2}{\partial x^2} + \frac{\partial^2}{\partial y^2} + 1 \right) \phi = 0, \quad 0 \leq y \leq h, \quad -\infty < x < \infty \quad (12)$$

$$\phi_y(x, 0) = 0, \quad (13)$$

$$\left\{ \frac{\partial^4}{\partial x^4} - \mu^4(x) \right\} \phi_y(x, h) = \alpha(x) \phi(x, h), \quad (14)$$

$$\phi(x, y) = \begin{cases} (Ae^{i\eta_0 x} + R_0 e^{-i\eta_0 x}) \cosh(\tau_0 y) & \text{as } x \rightarrow -\infty, \\ T_0 \cosh(\lambda_0 y) e^{i\nu_0 x} & \text{as } x \rightarrow +\infty, \end{cases} \quad (15)$$

where the second and third terms of the plate equation (9) are neglected under the assumptions stated above. These assumptions are discussed further in § 6. The plate wavenumber μ and fluid loading parameter α are defined by

$$\mu^4(x) = \left(\frac{\omega^2}{k^4} \right) \frac{m_1 + m_2 e^{x/a}}{B_1 + B_2 e^{x/a}}, \quad \alpha(x) = \left(\frac{\rho_0 \omega^2}{k^5} \right) \frac{1 + e^{x/a}}{B_1 + B_2 e^{x/a}}. \quad (16)$$

Each of these functions has a point of inflection, where the gradient is maximal, at $x = a \log(B_1/B_2)$. Small values of a represent a rapid transition near the points of inflection from the left-hand asymptotic values B_1 and m_1 to the right-hand ones B_2 and m_2 ; thus in the limit $a \rightarrow 0$, when the points of inflection tend to 0, the problem is equivalent to one of standard Wiener-Hopf type, provided that edge conditions are introduced at the position of the discontinuity of material properties. In the special case $B_1 = B_2$, $\alpha(x)$ is constant and no assumptions regarding the relative sizes of μ_j^4 and ka are needed since the second and third terms in (9) are zero for all values of a . Further details about the limiting cases $a \rightarrow 0$ for $B_1 = B_2$ and $B_1 \neq B_2$ are discussed in § 6.

A solution of the form

$$\phi(x, y) = \frac{1}{2\pi} \int_C \Phi(s, y) e^{-ixs} ds \quad (17)$$

is sought, where the wavenumber s is regarded as a complex variable and C is a contour extending from $-\infty$ to ∞ which is chosen so that $\phi(x, y)$ satisfies the radiation condition (15). The location of contour C is crucial to the analysis which follows; full details are given in § 4. It is clear that expression (17)

satisfies (12) provided that

$$\Phi_{yy}(s, y) - (s^2 - 1)\Phi(s, y) = 0. \quad (18)$$

Thus $\Phi(s, y)$ has the general form

$$\Phi(s, y) = A(s)e^{\gamma y} + B(s)e^{-\gamma y},$$

where $\gamma = (s^2 - 1)^{1/2}$. The boundary condition at the lower duct surface, that is (13), implies that $A(s) - B(s) = 0$, so that

$$\Phi(s, y) = 2A(s) \cosh(\gamma y).$$

For convenience $A(s)$ is re-cast as

$$A(s) = \frac{f(s)}{(s^4 - \mu_1^4)\gamma \sinh(\gamma h) - \alpha_1 \cosh(\gamma h)}$$

where μ_1 and α_1 are the limiting values of the plate wavenumber and fluid loading parameter as $x \rightarrow -\infty$, defined by taking the appropriate limits in (16) and given explicitly in (22). Consequently, (17) becomes

$$\phi(x, y) = \frac{1}{2\pi} \int_C \frac{f(s) \cosh(\gamma y) e^{-ixs} ds}{(s^4 - \mu_1^4)\gamma \sinh(\gamma h) - \alpha_1 \cosh(\gamma h)}, \quad (19)$$

where $f(s)$ is an unknown meromorphic function. The denominator of the integrand is the dispersion relation appropriate to the plate of uniform properties μ_1 and α_1 . Equation (19) satisfies the governing equation (12) and the boundary condition (13). The function $f(s)$ is determined by the need to satisfy (14) and (15), and is expected to reveal the properties of the transmitted and reflected modes.

4 Solution of the boundary value problem

In the expression (19) for the velocity potential, the function $f(s)$ and the contour C must be chosen so that the plate and radiation boundary conditions,

(14) and (15) are satisfied. Using the definitions of $\mu^4(x)$ and $\alpha(x)$ in (14),

$$B_1\phi_{yxxxx} - m_1\omega^2\phi_y - \rho_0\omega^2\phi + e^{x/a}(B_2\phi_{yxxxx} - m_2\omega^2\phi_y - \rho_0\omega^2\phi) = 0 \text{ for } y = h. \quad (20)$$

On substituting the inverse Fourier integral (19) for $\phi(x, y)$ into (20), it is found that

$$\begin{aligned} & \frac{1}{2\pi} \int_C \frac{f(s)\{B_1s^4\gamma \sinh(h\gamma) - m_1\omega^2\gamma \sinh(h\gamma) - \rho_0\omega^2 \cosh(h\omega)e^{-ixs}\}}{(s^4 - \mu_1^4)\gamma \sinh(h\gamma) - \alpha_1 \cosh(h\gamma)} ds \\ & + \frac{1}{2\pi} \int_C \frac{f(s)\{B_2s^4\gamma \sinh(h\gamma) - m_2\omega^2\gamma \sinh(h\gamma) - \rho_0\omega^2 \cosh(h\omega)e^{-ix(s+i/a)}\}}{(s^4 - \mu_1^4)\gamma \sinh(h\gamma) - \alpha_1 \cosh(h\gamma)} ds \\ & = 0. \end{aligned} \quad (21)$$

This imposes a further constraint on $f(s)$, that is $f(s)$ must be such that both the integrals exist. It is convenient to define.

$$K_j(s) = (s^4 - \mu_j^4)\gamma \sinh(h\gamma) - \alpha_j \cosh(h\gamma), \quad j = 1, 2, \quad (22)$$

where

$$\mu_j^4 = \frac{m_j\omega^2}{k^4 B_j}, \quad \alpha_j = \frac{\rho_0\omega^2}{k^5 B_j}.$$

Then (21) may be written as

$$\frac{B_1}{2\pi} \int_C f(s)e^{-ixs} ds + \frac{B_2}{2\pi} \int_C \frac{K_2(s)}{K_1(s)} f(s)e^{-ix(s+i/a)} ds = 0. \quad (23)$$

Provided there are no singularities of the integrand lying in the region between the contour C and the contour C' which is everywhere distant $1/a$ above C , the first term in (23) can be replaced by

$$\frac{B_1}{2\pi} \int_C f(s)e^{-ixs} ds = \frac{B_1}{2\pi} \int_{C'} f(s)e^{-ixs} ds = \frac{B_1}{2\pi} \int_C f\left(t + \frac{i}{a}\right) e^{-ix\left(t + \frac{i}{a}\right)} dt. \quad (24)$$

Then (23) becomes

$$\frac{B_1}{2\pi} \int_C f\left(s + \frac{i}{a}\right) e^{-ix\left(s + \frac{i}{a}\right)} ds + \frac{B_2}{2\pi} \int_C \frac{K_2(s)}{K_1(s)} f(s)e^{-ix\left(s + \frac{i}{a}\right)} ds = 0. \quad (25)$$

It follows that (23) will be satisfied if $f(s)$ satisfies the functional difference equation

$$\frac{f\left(s + \frac{i}{a}\right)}{f(s)} = -p(s), \quad p(s) = \frac{B_2 K_2(s)}{B_1 K_1(s)}. \quad (26)$$

There are infinitely many solutions to functional difference equations of this type. The precise form of $f(s)$ is dictated by the need to satisfy (15), ensure convergence of the integrals in (21) and be pole-free in the (not necessarily straight) strip lying between C and C' . The latter point is essential in view of (24) above. The choice of $f(s)$ is thus of paramount importance to the analysis. The solution of (26) is outlined below with further details given in Appendix A. For ease of exposition two special cases will be investigated. These are the simplest in that they have the smallest numbers of propagating modes in the scattered acoustic field. The conditions, expressed in terms of the intrinsic fluid loading parameter $\epsilon_1 = \epsilon_1(j) = \alpha_j/\mu_j^4$ denoted by ϵ in Cannell [4] and α in Crighton *et al* [6] ($j = 1, 2$), are

- i) each of the numerator and denominator of $p(s)$ has exactly one pair of real zeros; this requires $h < \pi/2$ and $\epsilon_1 < \tan h$;
- ii) each of the numerator and denominator of $p(s)$ has exactly two pairs of real zeros; this happens if either $h < \pi/2$ and $\epsilon_1 > \tan h$ or $3\pi/2 > h > \pi/2$ and $\epsilon_1 < \tan h$.

In (26), it is convenient to write $f(s) = f_0(s)f_1(s)f_2(s)$ so that (26) is equivalent to the three functional difference equations

$$\frac{f_0\left(s + \frac{i}{a}\right)}{f_0(s)} = -1, \quad (27)$$

$$\frac{f_1\left(s + \frac{i}{a}\right)}{f_1(s)} = \frac{B_2}{B_1} \quad (28)$$

and

$$\frac{f_2\left(s + \frac{i}{a}\right)}{f_2(s)} = \frac{K_2(s)}{K_1(s)}. \quad (29)$$

Solutions of (27) are anti-periodic functions, i.e. those which change sign when s is increased by i/a , for example $\sinh\{(2n-1)\pi as\}$. Functions of the form $c(s)e^{-ibs}$, where $b = a \log(B_2/B_1)$ and $c(s)$ is periodic with period i/a , satisfy (28). Here, the function $c(s)$ is disregarded, as it can be incorporated in the anti-periodic solution of (27). The expression e^{-ibs} will also be omitted in the subsequent analysis, as removing it from the velocity potential (19) merely has the effect of translating the y -axis a distance $a \log(B_2/B_1)$ away from the point of inflection of the functions μ^4 and α . Such a shift of coordinates does not affect the physical conclusions.

Equation (29) can be solved by writing $p(s)$ as an infinite product over its zeros and poles, which are denoted by $\pm\nu_n$ and $\pm\eta_n$, $n = 0, 1, 2, \dots$, respectively. Note that η_0 and ν_0 are real (together with η_1 and ν_1 in case (ii) above), and $\Re(\eta_n) \geq 0$, $\Re(\nu_n) \geq 0$, $n = 1, 2, 3, \dots$. Details of the solution method are given in Appendix A where it is shown that a solution is

$$f_2(s) = \prod_{n=0}^{\infty} \frac{\Gamma\{1 - ia(\eta_n - s)\}\Gamma\{-ia(\nu_n + s)\}}{\Gamma\{1 - ia(\nu_n - s)\}\Gamma\{-ia(\eta_n + s)\}}. \quad (30)$$

The poles of functions appearing in the integrand of (19), together with zeros of $f_2(s)$, are represented in Figure 4. A pole at $-\eta_0$, representing the incident wave, can be introduced by choosing

$$f_0(s) = \frac{H}{\sinh\{\pi a(s + \eta_0)\}}, \quad (31)$$

which satisfies (27). The constant H will be chosen later to give the incident wave the required amplitude, A in (15). The contour C of (19) is now chosen to pass below $\pm\eta_0$ and above $-\nu_0$. This choice ensures that $\phi(x, y)$ satisfies the radiation condition (15) and also permits the deformation detailed in (24).

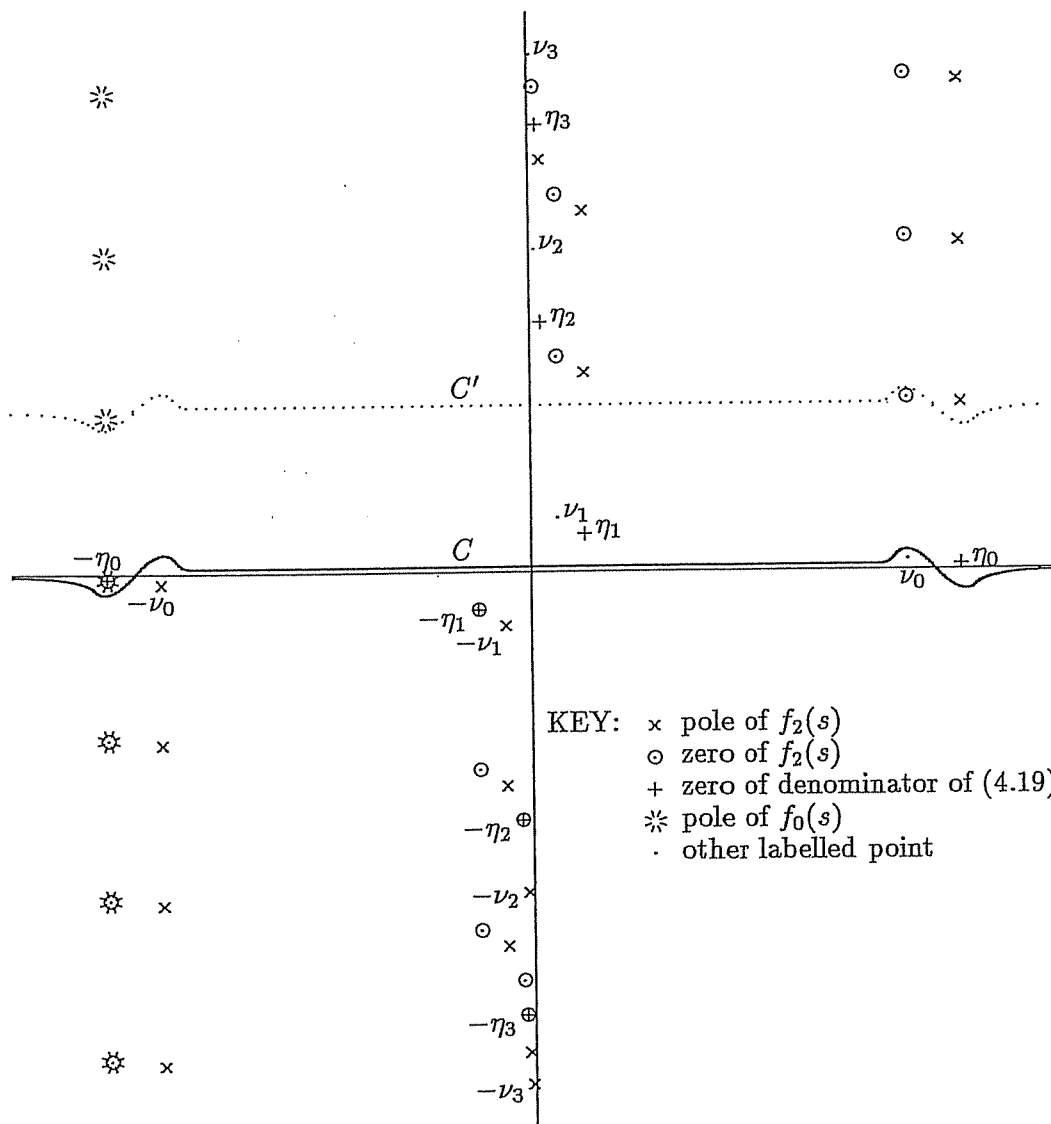


Figure 4: Complex s -plane showing poles of the integrand in (19) with the contours C and C'

That is, no singularities of $f(s)$ lie between the contours C and C' , as can be seen in Figure 4.

When the poles of the denominator of the integrand of (19) are taken into account, the modes which do not attenuate for $x \rightarrow \pm\infty$ are seen to be $-\eta_0$ (incident wave), $-\nu_0$ (transmitted wave) and η_0 (reflected wave). Further transmitted and reflected modes may be given by $-\nu_1, \eta_1$ etc. The complete solution to (26) is now

$$f(s) = \frac{-iH}{\pi} \cdot \frac{\Gamma\{1 + ia(s + \eta_0)\}\Gamma\{1 - ia(\eta_0 - s)\}\Gamma\{-ia(\nu_0 + s)\}}{\Gamma\{1 - ia(\nu_0 - s)\}} \times \prod_{n=1}^{\infty} \frac{\Gamma\{1 - ia(\eta_n - s)\}\Gamma\{-ia(\nu_n + s)\}}{\Gamma\{1 - ia(\nu_n - s)\}\Gamma\{-ia(\eta_n + s)\}}. \quad (32)$$

Expression (32) clearly contains three infinite families of poles given by

- i) $-\eta_0 + im/a; m = 0, 1, 2, \dots;$
- ii) $\eta_n + im/a; n = 0, 1, 2, \dots; m = 0, 1, 2, \dots;$
- iii) $-\nu_n - im/a; n = 0, 1, 2, \dots; m = 1, 2, \dots;$

and these are represented in Figure 4. It should be noted that $f(s)$ does not contain poles at $s = \pm\eta_0$ which correspond to the forcing term and its reflected wave. These terms are present in the denominator of the integral (19), that is they are zeros of $K_1(s)$. It is clear that the integral (24) is free of poles in the strip $0 \leq \Im(s) \leq 1/a$ provided the contour C passes above the pole at $-\nu_0$. In addition to these requirements, integral (19) will have the correct physical composition if and only if C passes below the poles $s = \pm\eta_0$ that arise due to $K_1(s)$.

It is shown in Appendix A that $f(s)$ decays exponentially for $s \rightarrow \infty$ in a horizontal strip. This allows the integral (19) to converge and provides the final justification for moving the contour in (23).

5 Reflection and transmission coefficients

The incident wave I is obtained by isolating the residue contribution from (19) at $-\eta_0$, on closing the contour in the upper half-plane, to get

$$I = \frac{if(-\eta_0)}{K_1'(-\eta_0)} \cosh(\tau_0 y) e^{i\eta_0 x}, \quad (33)$$

where $K_1(s)$ is defined in (22). The incident amplitude A in (15) is, by comparison with (19),

$$A = \frac{if(-\eta_0)}{K_1'(-\eta_0)}. \quad (34)$$

Hence, the constant H is related to A by

$$\begin{aligned} H &= \pi A K_1'(-\eta_0) \frac{\Gamma\{1 - ia(\nu_0 + \eta_0)\}}{\Gamma(1 - 2ia\eta_0)\Gamma\{-ia(\nu_0 - \eta_0)\}} \\ &\times \prod_{n=1}^{\infty} \frac{\Gamma\{1 - ia(\nu_n + \eta_0)\}\Gamma\{-ia(\eta_n - \eta_0)\}}{\Gamma\{1 - ia(\eta_n + \eta_0)\}\Gamma\{-ia(\nu_n - \eta_0)\}}. \end{aligned} \quad (35)$$

The notation $\tau_n = \gamma(\eta_n)$, $\lambda_n = \gamma(\nu_n)$ is used here, and defines the wavenumbers τ_0 and λ_0 which were used in dimensional form in § 3.

The first reflected mode is given by the residue contribution at η_0 , the contour being closed in the upper half-plane; thus

$$R_0 = \frac{f(\eta_0)}{K_1'(\eta_0)} \quad (36)$$

and

$$|R_0| = \left| \frac{f(\eta_0)}{K_1'(\eta_0)} \right|. \quad (37)$$

To relate this to (34), note that $K_1'(-s) = -K_1'(s)$ since $K_1(s)$ is an even function, so that

$$\begin{aligned} \left| \frac{R_0}{A} \right| &= \left| \frac{f(\eta_0)}{f(-\eta_0)} \right| \\ &= \left| \frac{\Gamma(2ia\eta_0)}{\Gamma(-2ia\eta_0)} \right| \left| \frac{\sinh\{a\pi(\nu_0 - \eta_0)\}}{\sinh\{a\pi(\nu_0 + \eta_0)\}} \right| \\ &\times \prod_{n=1}^{\infty} \left| \frac{\sinh\{a\pi(\eta_n + \eta_0)\} \sinh\{a\pi(\nu_n - \eta_0)\}}{\sinh\{a\pi(\eta_n - \eta_0)\} \sinh\{a\pi(\nu_n + \eta_0)\}} \right|. \end{aligned} \quad (38)$$

On the right-hand side the first factor is 1 provided that η_0 is real, and the second factor is less than one for all a . The infinite product is 1 if η_n and ν_n are purely imaginary. This is also true if a pair of roots have the form $\eta_n = iz$, $\eta_{n+1} = i\bar{z}$ which will occur for $\alpha \gg 1$. This leads to the alternative forms

$$\left| \frac{R_0}{A} \right| = \begin{cases} \left| \frac{\sinh\{a\pi(\nu_0 - \eta_0)\}}{\sinh\{a\pi(\nu_0 + \eta_0)\}} \right|, & \eta_0, \nu_0 \in \mathfrak{R}, \\ \left| \frac{\sinh\{a\pi(\nu_0 - \eta_0)\} \sinh\{a\pi(\eta_1 + \eta_0)\} \sinh\{a\pi(\nu_1 - \eta_0)\}}{\sinh\{a\pi(\nu_0 + \eta_0)\} \sinh\{a\pi(\eta_1 - \eta_0)\} \sinh\{a\pi(\nu_1 + \eta_0)\}} \right|, & \\ \eta_0, \eta_1, \nu_0, \nu_1 \in \mathfrak{R}. \end{cases} \quad (39)$$

which are valid for cases (i) and (ii) respectively (see §. 4). In the limit as $a \rightarrow 0$, the first of the above expressions, valid for case (i), becomes

$$\left| \frac{R_0}{A} \right| = \left| \frac{\eta_0 - \nu_0}{\eta_0 + \nu_0} \right|, \quad (40)$$

which agrees with the reflection coefficient derived from the solution of the limiting Wiener-Hopf problem with continuous edge conditions. In the limit as $a \rightarrow \infty$, the first expression in (39) tends to zero. This indicates that, even though there may be a substantial difference between the left and right asymptotic bending stiffnesses or thicknesses, the reflected wave has negligible amplitude provided that the material properties change slowly enough.

The first transmitted mode is given by the residue contribution at $-\nu_0$, the contour being closed in the lower half-plane, so that its amplitude is

$$T_0 = \frac{\text{Res}_{s=-\nu_0} f(s)}{K_1(-\nu_0)}, \quad (41)$$

where the residue can be expressed as an infinite product by means of (32),

$$\begin{aligned} \text{Res}_{s=-\nu_0} f(s) &= \frac{H}{a\pi} \cdot \frac{\Gamma\{1 + ia(\eta_0 - \nu_0)\} \Gamma\{1 - ia(\eta_0 + \nu_0)\}}{\Gamma(1 - 2ia\nu_0)} \\ &\times \prod_{n=1}^{\infty} \frac{\Gamma\{1 - ia(\eta_n + \nu_0)\} \Gamma\{-ia(\nu_n - \nu_0)\}}{\Gamma\{1 - ia(\nu_n + \nu_0)\} \Gamma\{-ia(\eta_n - \nu_0)\}}. \end{aligned} \quad (42)$$

CHAPTER 4. SMOOTHLY-VARYING BENDING

The above, together with the expression for H in (35), give T_0 in terms of the gamma function and, for case (i), the limiting forms for small and large a satisfy

$$\lim_{a \rightarrow 0} \left| \frac{T_0}{A} \right| = \frac{2\eta_0}{\nu_0 + \eta_0} \prod_{n=1}^{\infty} \left| \frac{\eta_n - \eta_0}{\eta_n - \nu_0} \cdot \frac{\nu_n + \eta_0}{\nu_n + \nu_0} \right| \quad (43)$$

and

$$\lim_{a \rightarrow \infty} \left| \frac{T_0}{A} \right| = \sqrt{\frac{\eta_0}{\nu_0}} \prod_{n=1}^{\infty} \left| \frac{\eta_n - \eta_0}{\eta_n - \nu_0} \cdot \frac{\nu_n + \eta_0}{\nu_n + \nu_0} \right|. \quad (44)$$

The first of these expressions agrees with the transmission coefficient derived from the Wiener-Hopf problem mentioned above. It is interesting to note that, whilst $|R_0/A| \rightarrow 0$ as $a \rightarrow \infty$, there is no simple form for T_0 in this limit. This is to be expected, since the different wavenumbers of the transmitted and incident modes would require different amplitudes to convey the same energy.

The following graphs show the moduli of the fundamental reflection and transmission coefficients for the cases $B_1 = B_2$ and $B_1 \neq B_2$. In the first case the graphs are valid for $a \geq 0$ but for the case $B_1 \neq B_2$ this is not so. Figure 5 compares the modulus of the reflection coefficient for $\mu_1 = 0.5$, $\mu_2 = 3.5$ and $\alpha_1 = \alpha_2 = 200$ against the heavy fluid loading case in which $\mu_1 = 5$, $\mu_2 = 15$ and $\alpha_1 = \alpha_2 = 100000$. It is clear, with reference to equation (39), that both curves decay exponentially with increasing a , however, although initially larger in magnitude the reflection coefficient for the second set of parameters decays significantly more rapidly. Figure 6 shows the modulus of the transmission coefficient for the same two sets of parameters. It is clear that the two curves are very nearly constant albeit at different values. Figure 7 compares the modulus of the reflection coefficient for $\mu_1 = 1.5$, $\mu_2 = 3$ and $\alpha_1 = 200$, $\alpha_2 = 1500$ against that for $\mu_1 = 5$, $\mu_2 = 15$ and $\alpha_1 = 1000$, $\alpha_2 = 100000$. In this case the graph is valid only for $a > 0.3$ and it is clear that both curves are extremely small for $a = O(1)$. The transmission coefficient, for the same two sets of parameters, is shown in Figure 8 and, clearly, for $a > 0.3$ the curves are constant. From Fig-

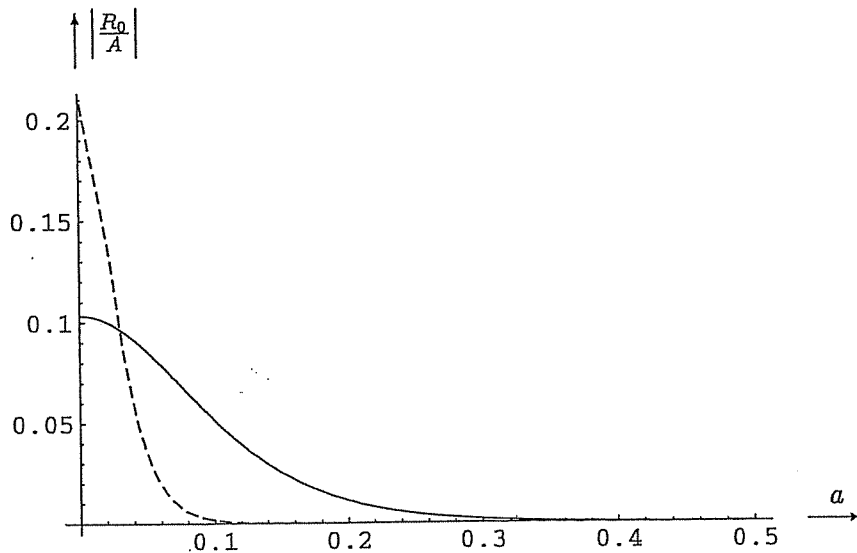


Figure 5: The modulus of the reflection coefficient for the case $B_1 = B_2$; continuous line is for $\mu_1 = 0.5$, $\mu_2 = 3.5$, $\alpha_1 = \alpha_2 = 200$ and broken line is for $\mu_1 = 5$, $\mu_2 = 15$ and $\alpha_1 = \alpha_2 = 100000$

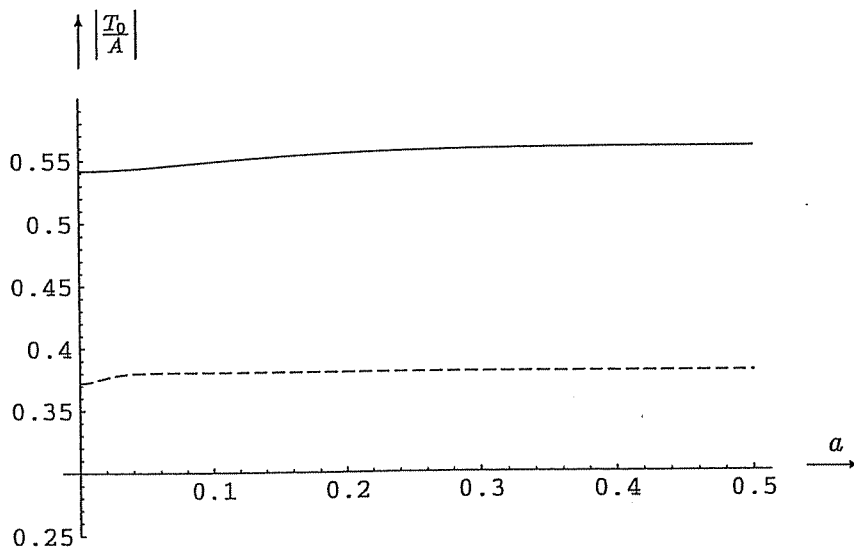


Figure 6: The modulus of the transmission coefficient, evaluated on $y = h$, for the case $B_1 = B_2$; continuous line is for $\mu_1 = 0.5$, $\mu_2 = 3.5$, $\alpha_1 = \alpha_2 = 200$ and broken line is for $\mu_1 = 5$, $\mu_2 = 15$ and $\alpha_1 = \alpha_2 = 100000$

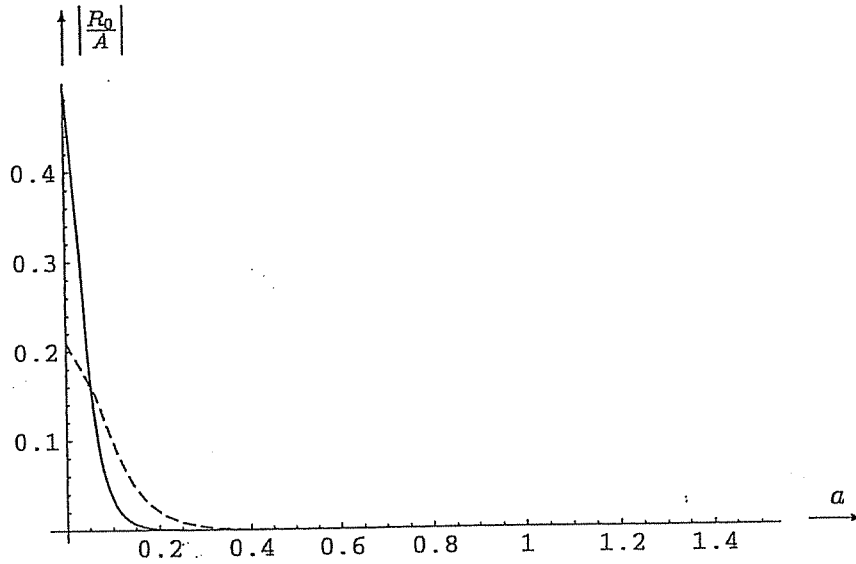


Figure 7: The modulus of the reflection coefficient for the case $B_1 \neq B_2$; continuous line is for $\mu_1 = 1.5$, $\mu_2 = 3$, $\alpha_1 = 200$, $\alpha_2 = 1500$ and broken line is for $\mu_1 = 5$, $\mu_2 = 15$ and $\alpha_1 = 1000$, $\alpha_2 = 100000$

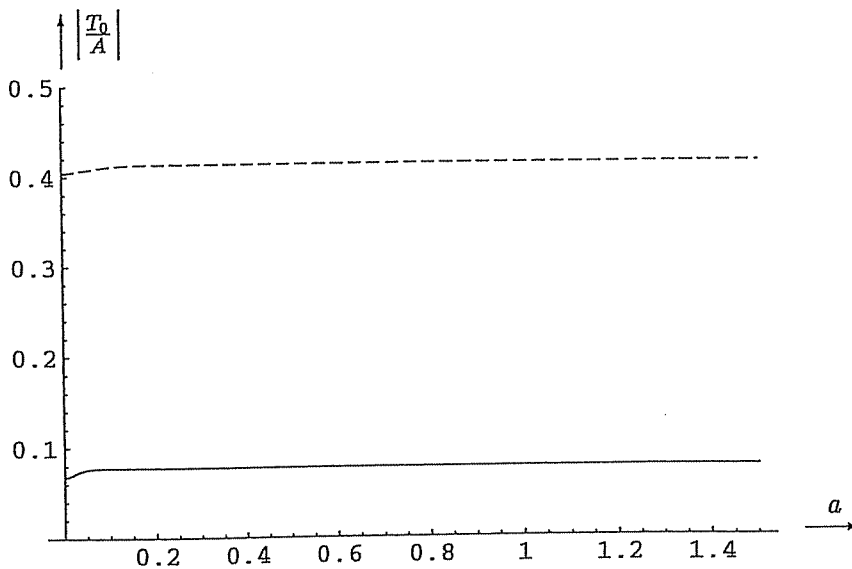


Figure 8: The modulus of the transmission coefficient, evaluated on $y = h$, in the case $B_1 \neq B_2$; continuous line is for $\mu_1 = 1.5$, $\mu_2 = 3$, $\alpha_1 = 200$, $\alpha_2 = 1500$ and broken line is for $\mu_1 = 5$, $\mu_2 = 15$ and $\alpha_1 = 1000$, $\alpha_2 = 100000$

ures 5–8 it is clear that the most interesting behaviour for both the reflection and transmission coefficients occurs for $a \ll 1$. The discussion of section 6 centres on a number of different approximations to the full plate equation (9) and, in particular, presents a modified version by which results valid for $B_1 \neq B_2$, $a \ll 1$ may be obtained.

6 Discussion and Conclusions

The analysis of § 3 and § 4 involves a simplified plate equation, (14), which is valid for $|B'/B|, |B''/B| \ll \mu_j^4, \alpha_j, j = 1, 2$ and also for the case $B_1 = B_2$. In this section an alternative modification is presented by which results can be obtained for the cases where (14) is not valid and, in particular, for $a \ll 1$.

The non-dimensional form of the full plate equation (9) is

$$\left\{ \frac{\partial^4}{\partial x^4} + \frac{2B'(x)}{B(x)} \frac{\partial^3}{\partial x^3} + \frac{B''(x)}{B(x)} \frac{\partial^2}{\partial x^2} - \mu^4(x) \right\} \phi_y - \alpha(x)\phi = 0, \quad -\infty < x < \infty, \\ y = h. \quad (45)$$

For situations in which the constraints discussed above do not apply the *ansatz* of § 3 can still be applied to the full plate equation. It is found that

$$\begin{aligned} & \frac{1}{2\pi} \int_C f(s) e^{-ixs} ds + \frac{1}{\pi} \int_C f(s) e^{-ix(s+i/a)} ds \\ & + \frac{1}{\pi} \int_C \frac{B_2 K_2(s)}{B_1 K_1(s)} f(s) e^{-ix(s+2i/a)} ds + \frac{1}{2\pi} \int_C \frac{B_2 K_2(s)}{B_1 K_1(s)} f(s) e^{-ix(s+3i/a)} ds \\ & + \frac{B_2 - B_1}{\pi a^2} \int_C \frac{s^2 (2ias + 1) \gamma \sinh(h\gamma) f(s) e^{-ix(s+i/a)}}{B_1 K_1(s)} ds \\ & + \frac{B_2 - B_1}{2\pi a^2} \int_C \frac{s^2 (2ias - 1) \gamma \sinh(h\gamma) f(s) e^{-ix(s+2i/a)}}{B_1 K_1(s)} ds \\ & = 0, \end{aligned} \quad (46)$$

where $f(s)$ is the unknown (meromorphic) function contained in the integral representation for $\phi(x, y)$ and the contour C extends from $-\infty$ to $+\infty$ but its full

specification is not yet known. In order to obtain a (rather more complicated) functional difference equation from (46) it is necessary for all but one of the integrals to shift the path of integration upward a distance m/a , where $m = 1, 2, 3$ depending on the exponent in the integrand. Then the substitution $s = t + im/a$ ensures that each final integral contains the factor $e^{-ix(t+3i/a)}$. The contour C , which can be suitably translated without encountering poles of the integrand, is similar to that shown in Figure 4, but with extra detours below the points $-\eta_0, \eta_0, \eta_1$ etc. Such a contour is possible if $2\Im(\eta_1) > 3/a$, that is if a is suitably large. Otherwise, allowance has to be made for poles which are the wrong side of the contour by adding appropriate residue terms to the right-hand side of (46). For $a = O(1)$ or $a \ll 1$ a contour can be found only if η_1, η_2 etc have small real parts as indicated in Figure 4. This can be ensured if the wavenumber k is assumed to have a small positive imaginary part as may be seen easily for extreme values of α_1 or α_2 , when $\hat{\eta}_l$ and $\hat{\nu}_l$ take the forms

$$\hat{\eta}_n, \hat{\nu}_n \sim \begin{cases} \sqrt{k^2 - \frac{\pi^2 n^2}{k^2 \hat{h}^2}} & (\alpha_j \rightarrow 0; j = 1, 2), \\ \sqrt{k^2 - \frac{\pi^2 (n - 1/2)^2}{k^2 \hat{h}^2}} & (\alpha_j \rightarrow \infty). \end{cases}$$

Positive imaginary values of the above expressions acquire small real parts when k is given a small positive imaginary part. There is no loss of generality involved in this assumption provided that $\Im(k) \rightarrow 0$ at the end of the analysis.

The full difference equation for $f(s)$ is now

$$\begin{aligned} & \frac{B_2 K_2(s)}{B_1 K_1(s)} f(s) + \frac{2B_2 K_2(s + i/a)}{B_1 K_1(s + i/a)} f\left(s + \frac{i}{a}\right) + f\left(s + \frac{i}{a}\right) \\ & + \frac{B_2 K_2(s + 2i/a)}{B_1 K_1(s + 2i/a)} f\left(s + \frac{2i}{a}\right) + 2f\left(s + \frac{2i}{a}\right) + f\left(s + \frac{3i}{a}\right) \\ & + \frac{\{s + 3i/(2a)\}(s + i/a)^2 \{B_2 K_2(s + i/a) - B_1 K_1(s + i/a)\}}{\pi a^2 \{(s + i/a)^4 - \sigma^4\} B_1 K_1(s + i/a)} f\left(s + \frac{i}{a}\right) \\ & + \frac{\{s + 3i/(2a)\}(s + 2i/a)^2 \{B_2 K_2(s + 2i/a) - B_1 K_1(s + 2i/a)\}}{2\pi a^2 \{(s + 2i/a)^4 - \sigma^4\} B_1 K_1(s + 2i/a)} f\left(s + \frac{2i}{a}\right) \end{aligned}$$

$$= 0, \quad (47)$$

where σ is defined by

$$\sigma^4 = \frac{m_2 - m_1}{B_2 - B_1}.$$

The quantity σ plays an important role in the Wiener-Hopf analysis, see [3].

When $\hat{a} \gg 1$, the first six terms on the left-hand side predominate, forming a third-order functional difference equation, that is

$$\begin{aligned} p(s)f(s) + f\left(s + \frac{i}{a}\right) + 2p\left(s + \frac{i}{a}\right)f\left(s + \frac{i}{a}\right) + 2f\left(s + \frac{2i}{a}\right) \\ + p\left(s + \frac{2i}{a}\right)f\left(s + \frac{2i}{a}\right) + f\left(s + \frac{3i}{a}\right) = 0, \end{aligned} \quad (48)$$

where $p(s)$ denotes $B_2K_2(s)/\{B_1K_1(s)\}$. This can be re-cast as

$$F(s) + 2F(s + i/a) + F(s + 2i/a) = 0 \quad (49)$$

where

$$p(s)f(s) + f(s + i/a) = F(s).$$

Its is easily shown that

$$F(s) = \{A(s) + sB(s)\}e^{\pi sa}$$

where the functions $A(s)$ and $B(s)$ are periodic so that, for example, $A(s) = A(s + i/a)$. The solution to (48) that has the correct pole structure and for which the integral representation of the velocity potential $\phi(x, y)$ exists is obtained only if $A(s) = B(s) = 0$ whence the results of § 4 are retrieved. For $\hat{a} \ll 1$, the last two terms on the left-hand side of (47) appear to predominate, but the limiting equation does not provide physically meaningful solutions. This is because the difference between the arguments s and $s + i/a$ tends to infinity as a tends to zero, with the result that the limiting equation no longer has the nature of a difference equation. The increasingly abrupt change in physical properties

as $a \rightarrow 0$ invalidates assumptions on which the thin plate theory are based. A more productive approach for analysis of the problem when $a \ll 1$ is to multiply (9) throughout by $B(x)$ and then replace the quantities $B'(x)$ and $B''(x)$ by the generalised functions which reflect their limiting properties. The notation $B(x) = B(x; a)$ makes the parameter explicit. It is shown in Appendix C that

$$\lim_{n \rightarrow \infty} B'(x; 1/n) = (B_2 - B_1)\delta(x) \quad (50)$$

and

$$\lim_{n \rightarrow \infty} B''(x; 1/n) = (B_2 - B_1)\delta'(x) \quad (51)$$

where $\delta(x)$ here denotes the Dirac delta function. The analysis presented herein is based on the assumption that the velocity potential maintains continuity of displacement, gradient and the next two derivatives with respect to x across $x = 0$, that is

$$\begin{aligned} \phi_y(0-, h) &= \phi_y(0+, h), \\ \phi_{yx}(0-, h) &= \phi_{yx}(0+, h), \\ \phi_{yxx}(0-, h) &= \phi_{yxx}(0+, h), \\ \phi_{yxxx}(0-, h) &= \phi_{yxxx}(0+, h). \end{aligned} \quad (52)$$

Under these conditions and for $a \ll 1$, the terms of interest give rise to forcing functions

$$2B'(x) \frac{\partial^3 \phi_y(x, h)}{\partial x^3} \sim 2(B_2 - B_1)\phi_{yxxx}(x, h)\delta(x) = -A_0\delta(x) \quad (53)$$

say and

$$B''(x) \frac{\partial^2 \phi_y(x, h)}{\partial x^2} \sim (B_2 - B_1)\phi_{yxx}(x, h)\delta'(x) = -A_1\delta'(x). \quad (54)$$

The boundary condition (14) is then replaced by

$$\left\{ B(x) \frac{\partial^4}{\partial x^4} - m(x) \right\} \phi_y(x, h) - \rho_0 \omega^2 \phi(x, h) = A_0\delta(x) + A_1\delta'(x). \quad (55)$$

Equation (3.55) permits the theory presented here to be extended to two further situations. Firstly, it approximates the plate boundary condition for the case $B_1 \neq B_2$ with $a \ll 1$. Secondly, it models the case $B_1 = B_2$, $a > 0$ with the plate constrained so that its displacement and gradient are continuous but specified at $x = 0$ (or at any other x value). In the latter case, the delta functions on the right-hand side of (3.54) are to be viewed as forcing terms (cf [2]) and are not the $a \rightarrow 0$ limiting forms of B' and B'' (which are in any case known to be zero for $B_1 = B_2$). Both situations are of interest and the solution of the boundary value problem with (3.55) instead of (3.9) as boundary condition could form the subject of future research. It was noted in § 3 that $B' = B'' = 0$ for $B_1 = B_2$. Expressions (3.53) and (3.54) are consistent with this since then $A_1 = A_0 = 0$. This special case in which $B_2 = B_1$ arises if the Young's modulus and Poisson's ratio vary with x but $\delta(x)$ also varies in such a way that

$$\frac{E(x)\delta(x)^3}{12(1-\nu(x)^2)} = \text{constant}.$$

It is worthwhile commenting on the Wiener-Hopf problem which arises as $a \rightarrow 0$. On multiplying (4.9) through by $B(x)$ and taking this limit in each term it is found that

$$\left[\{B_1 + (B_2 - B_1)H(x)\} \frac{\partial^4}{\partial x^4} - \{m_1 + (m_2 - m_1)H(x)\} \right] \phi_y(x, h) - \rho_0 \omega^2 \phi(x, h) = A_0(x)\delta(x) + A_1(x)\delta'(x) \quad (3.56)$$

where $H(x)$ is the Heaviside step function. The boundary value problem that is obtained on replacing (3.14) with this two-part condition can be solved by recourse to the Wiener-Hopf technique. It should be noted that this is not the Wiener-Hopf problem that is referred to and used for comparison in § 5. The Wiener-Hopf problem results quoted there arise from the $a \rightarrow 0$ limiting case of (3.14), that is, the Wiener-Hopf limit of the $a \gg 1$ approximation to (3.9).

Thus, the results presented

in § 5 for the case $B_1 \neq B_2$, although not valid for $a = 0$, are compared with the Wiener-Hopf result as a means of checking algebraic accuracy. The results are, however, valid for $a = 0$ in the case $B_1 = B_2$.

As a final point, it is noted that the special case $m_1 = m_2$ permits some slight simplification of the functional difference equation. This case arises if the density and thickness of the plate material both vary but in such a way that the area density $m = \rho_0 \delta$ remains uniform. In this case the quantity σ in (47) is zero.

References

- [1] Abrahams, I.D. (1986) “*Diffraction by a semi-infinite membrane in the presence of a vertical barrier. I*” *Sound Vib.* **111**, 191-207.
- [2] Abrahams, I. D. & Lawrie, J. B. (1995) “*Travelling waves on a membrane: reflection and transmission at a corner of arbitrary angle. I*” *Proc. R. Soc.* **A451**, 657-683.
- [3] Brazier-Smith, P.R. (1987) “*The acoustic properties of two co-planar half plates*” *Proc. R. Soc. A* **409**, 115-139.
- [4] Cannell, P.A.(1975) ‘*Edge scattering of aerodynamic sound by a lightly loaded elastic half plane*’. *Proc. R. Soc.* **A347**, 213-238.
- [5] Cannell, P. A. (1976) “*Acoustic edge scattering by a heavily loaded elastic half plane*” *Proc. R. Soc.* **A350**, 71-89.
- [6] Crighton, D. G., Dowling, A. P. Ffowes Williams, J. E. Heckl, M. & Leppington, F. G. *Modern Methods in Analytical Acoustics* (Springer, London 1992).
- [7] Evans, D. V. (1985) “*A solution of a class of boundary-value problems with smoothly-varying boundary conditions*” *Q. Jl Mech. appl. Math.* **38**, 521-536.
- [8] Fernyhough, M. & Evans, D. V. (1996) “*Comparison of a step approximation to an exact solution of acoustic scattering in a uniform-width pipe with nonuniform wall impedance*” *Q. Jl Mech. appl. Math.* **49**, 419-437.
- [9] Lighthill, M.J. (1980) “*An introduction to Fourier analysis and generalised functions*” Cambridge University Press. ISBN 0 521 09128 4
- [10] Milne-Thomson, L. M. (1933) “*The Calculus of Finite Differences*” Macmillan, London.

- [11] Norris, A. N. & Wickham, G. R. (1995) "*Acoustic diffraction from the junction of two flat plates*" *Proc. R. Soc.* **A451**, 631-655.
- [12] Olver, F. W. J. (1974) "*Asymptotics and Special Functions* Academic Press, New York.
- [13] Osipov, A. V. & Norris, A. N. (1997) "*Acoustic diffraction by a fluid-loaded membrane corner*" *Proc. R. Soc.* **A453**, 43-64.
- [14] Rawlins, A. D. (1999) "*Diffraction by, or diffusion into a penetrable wedge*" *Proc. R. Soc.* **A455**, 2655-2686.
- [15] Roseau, M. "*Asymptotic Wave Theory*" (1976) North-Holland, Amsterdam.
- [16] Timoshenko, S. & Woinowsky-Krieger, S. (1959) "*Theory of Plates and Shells* McGraw-Hill, New York .
- [17] Warren, D.P., Lawrie, J.B. and Mohamed, I.M. (2002) "*Acoustic scattering in waveguides with discontinuities in height and material property*" *Wave Motion*, **36**, 119-142.

Appendix A

The functional difference equation

$$\frac{f(z+1)}{f(z)} = h(z) = h_1(z)h_2(z) \quad (\text{A.1})$$

has the formal solution

$$f(z) = \frac{\prod_{n=1}^{\infty} h_1(z-n)}{\prod_{n=0}^{\infty} h_2(z+n)} = \frac{1}{h_2(z)} \prod_{n=1}^{\infty} \frac{h_1(z-n)}{h_2(z+n)}, \quad (\text{A.2})$$

as may be seen by substituting and treating infinite products as absolutely convergent. The numerator and denominator in (A.2) are both adapted from Nörlund's *principal solution* [16]. In a particular case, $h_1(z)$ and $h_2(z)$ need to be chosen so that the solution given by (A.2) contains an absolutely convergent infinite product which defines a meromorphic functional solution to (A.1).

For the functional difference equation (29), suitable functions $h_1(s)$ and $h_2(s)$ can be defined in much the same way as the plus and minus functions employed in the Wiener-Hopf method. A product representation of $p(s)$, which is defined by (.26), is

$$p(s) = p(0) \prod_{n=0}^{\infty} \frac{1 - s^2/\nu_n^2}{1 - s^2/\eta_n^2}, \quad (\text{A.3})$$

where

$$p(0) = \frac{\mu_2^4 \tan h - \alpha_2}{\mu_1^4 \tan h - \alpha_1} = \prod_{n=0}^{\infty} \frac{\nu_n^2}{\eta_n^2}, \quad (\text{A.4})$$

the last equality following from the fact that $\lim_{s \rightarrow \infty} p(s) = 1$, which may be deduced from (26). The infinite product in (A.3) converges because both ν_n and η_n are asymptotically $\pi in/h$ as $n \rightarrow \infty$. The infinite product in (A.4) converges because $\nu_n - \eta_n = O(n^{-5})$, which follows from (B.7). Separating the zeros and poles of $p(s)$ into two sets, $\{\eta_n\} \cup \{\nu_n\}$ and $\{-\eta_n\} \cup \{-\nu_n\}$, $p(s)$ can be factorised as $p(s) = h_1(s)h_2(s)$, where

$$h_1(s) = \sqrt{p(0)} \prod_{n=0}^{\infty} \frac{1 - s/\nu_n}{1 - s/\eta_n}, \quad h_2(s) = \sqrt{p(0)} \prod_{n=0}^{\infty} \frac{1 + s/\nu_n}{1 + s/\eta_n}. \quad (\text{A.5})$$

The products converge absolutely for all s because, using (B.7) and (B.6), $\nu_n^{-1} - \eta_n^{-1} = O(n^{-7})$ as $n \rightarrow \infty$.

By (A.2), (29) has a solution

$$f_2(s) = \frac{1}{h_2(s)} \prod_{m=1}^{\infty} \frac{h_1\left(s - \frac{im}{a}\right)}{h_2\left(s + \frac{im}{a}\right)},$$

provided that the product converges. With $h_1(s)$ $h_2(s)$ are given by (A.5), the product does converge and can be reduced to the form

$$f_2(s) = \prod_{n=0}^{\infty} \frac{\Gamma\{1 - ia(\eta_n - s)\} \Gamma\{-ia(\nu_n + s)\}}{\Gamma\{1 - is(\nu_n - s)\} \Gamma\{-ia(\eta_n + s)\}} \quad (\text{A.6})$$

where the infinite product representation for $\Gamma(z)$ has been utilised. In order to examine the behaviour of $f(s)$ as $|s| \rightarrow \infty$ it is useful to recast $f_2(s)$ as

$$f_2(s) = \frac{1}{h_2(s)} \prod_{m=1}^{\infty} \prod_{n=0}^{\infty} \left(\frac{1 - \frac{s}{\eta_n + \frac{im}{a}}}{1 - \frac{s}{\nu_n + \frac{im}{a}}} \cdot \frac{1 + \frac{s}{\nu_n + \frac{im}{a}}}{1 + \frac{s}{\eta_n + \frac{im}{a}}} \right) \quad (\text{A.7})$$

$$= \frac{1}{h_2(s)} \prod_{k=0}^{\infty} \left(\frac{1 - s/y_k}{1 - s/x_k} \cdot \frac{1 + s/x_k}{1 + s/y_k} \right), \quad (\text{A.8})$$

where x_k (with $k = 0, 1, 2, \dots$) are the numbers $\nu_n + im/a$ arranged in order of increasing imaginary part and y_k are the numbers $\eta_n + im/a$ similarly arranged.

Note that

$$\left. \begin{aligned} |x_k| &\sim \sqrt{2\pi k/ha} && \text{as } k \rightarrow \infty, \\ |y_k| &\sim \sqrt{2\pi k/ha} && \text{as } k \rightarrow \infty, \\ x_k - y_k &= O(k^{-7/2}) && \text{as } k \rightarrow \infty. \end{aligned} \right\} \quad (\text{A.9})$$

The complete solution to (26) can now be written in the form

$$f(s) = \frac{He^{-ibs}}{h_2(s) \sinh\{\pi a(s + \nu_0)\}} \prod_{k=0}^{\infty} \left(\frac{1 - s/y_k}{1 - s/x_k} \cdot \frac{1 + s/x_k}{1 + s/y_k} \right). \quad (\text{A.10})$$

The roots η_n and ν_n become purely imaginary and increasing in modulus for large n . It follows that x_k and y_k are both purely imaginary for all large enough k , and so the infinite product and the function $h_2(s)$ in (A.10) are bounded as $s \rightarrow \infty$ in a horizontal strip. The complete function $f(s)$ therefore decays exponentially for such s , provided that $B_1 < e^\pi B_2$, and certainly if the factor e^{ibs} is omitted, as explained in § 4.

Appendix B

Let $\pm\eta_n$ be the roots of $K_1(s) = (s^4 - \mu_1^4)\gamma \tanh(\gamma h) - \alpha_1 = 0$, and $\pm\nu_n$ those of $K_2(s) = (s^4 - \mu_2^4)\gamma \tanh(\gamma h) - \alpha_2 = 0$. Apart from a finite number, say $2m_1$ and $2m_2$, the roots of each equation are purely imaginary. So for large n , η_n and ν_n are those roots which are closest to $\pi i(n - m_j + 1)/h$ respectively ($j = 1, 2$). In what follows it can be assumed without loss of generality that $m_1 = m_2 = m$.

An asymptotic expression for η_n in powers of n^{-1} can be obtained by the method given by Olver [12]. For simplicity of notation expressions are derived for the case $m = 1$. Using the notation $\tau_n = \gamma(\eta_n)$, define

$$\epsilon_n = h\tau_n + \pi in \quad (\text{B.1})$$

and write the defining equation as

$$\epsilon_n = \tanh^{-1} \frac{\alpha_1}{(\eta_n^4 - \mu_1^4)\tau_n}. \quad (\text{B.2})$$

From (B.1),

$$\epsilon_n = -h\eta_n \left(1 - \frac{1}{\eta_n^2}\right)^{\frac{1}{2}} + \pi in,$$

choosing an appropriate branch of γ ,

$$= -h\eta_n + \pi in + \frac{h}{2\eta_n} + \frac{h}{8\eta_n^3} + \frac{h}{16\eta_n^5} + \frac{5h}{128\eta_n^7} + \frac{7h}{256\eta_n^9} + \frac{21h}{1024\eta_n^{11}}$$

$$+ O(\eta_n^{-13}) \text{ as } n \rightarrow \infty. \quad (\text{B.3})$$

On the other hand, from (B.2),

$$\begin{aligned} \epsilon_n &= \tanh^{-1} \left\{ -\frac{\alpha_1}{\eta_n^5} \left(1 - \frac{\mu_1^4}{\eta_n^4}\right)^{-1} \left(1 - \frac{1}{\eta_n^2}\right)^{-\frac{1}{2}} \right\} \\ &= -\frac{\alpha_1}{\eta_n^5} - \frac{\alpha_1}{2\eta_n^7} - \frac{\alpha_1}{\eta_n^9} \left(\mu_1^4 + \frac{3}{8}\right) - \frac{\alpha_1}{\eta_n^{11}} \left(\frac{\mu_1^4}{2} + \frac{5}{16}\right) \\ &\quad + O(\eta_n^{-13}). \end{aligned} \quad (\text{B.4})$$

Combining (B.3) and (B.4),

$$\begin{aligned} h\eta_n &= \pi i n + \frac{h}{2\eta_n} + \frac{h}{8\eta_n^3} + \left(\frac{h}{16} + \alpha_1\right) \frac{1}{\eta_n^5} + \left(\frac{5h}{128} + \frac{\alpha_1}{2}\right) \frac{1}{\eta_n^7} \\ &\quad + \left(\frac{7h}{256} + \alpha_1\mu_1^4 + \frac{3\alpha_1}{8}\right) \frac{1}{\eta_n^9} + \left(\frac{21h}{1024} + \frac{\alpha_1\mu_1^4}{2} + \frac{5\alpha_1}{16}\right) \frac{1}{\eta_n^{11}} \\ &\quad + O(\eta_n^{-13}). \end{aligned} \quad (\text{B.5})$$

Starting with

$$\eta_n = \frac{\pi i n}{h} + O(n^{-1})$$

and repeatedly substituting for η_n in the right-hand side, the following expression is obtained

$$\begin{aligned} \eta_n &= \frac{\pi i n}{h} - \frac{i h}{2\pi n} - \frac{i h^3}{8\pi^3 n^3} - \left(\frac{1}{16} + \frac{\alpha_1}{h}\right) \frac{i h^5}{\pi^5 n^5} - \left(\frac{5}{128} + \frac{5\alpha_1}{2h}\right) \frac{i h^7}{\pi^7 n^7} \\ &\quad - \left\{ \frac{7}{256} + (\mu_1^4 + 4) \frac{\alpha_1}{h} \right\} \frac{i h^9}{\pi^9 n^9} + O(n^{-11}). \end{aligned} \quad (\text{B.6})$$

The expression for ν_n is the same except that α_2 and μ_2 replace α_1 and μ_1 . When $m > 1$, the expression on the right-hand side of (B.6) represents η_{n+m-1} or ν_{n+m-1} rather than η_n or ν_n . Subtracting,

$$\begin{aligned} \eta_{n+m-1} - \nu_{n+m-1} &= (\alpha_2 - \alpha_1) \frac{i h^4}{\pi^5 n^5} + (\alpha_2 - \alpha_1) \frac{5i h^7}{\pi^7 n^7} \\ &\quad + \{4(\alpha_2 - \alpha_1) + \mu_2^4 - \mu_1^4\} \frac{i h^9}{\pi^9 n^9} \\ &\quad + O(n^{-11}) \text{ as } n \rightarrow \infty. \end{aligned} \quad (\text{B.7})$$

Appendix C

The bending stiffness as a function of x is denoted by

$$B(x; a) = \frac{B_1 + B_2 e^{x/a}}{1 + e^{x/a}} \quad (\text{C.1})$$

where B_1 , B_2 and a are positive parameters and x is real. As $a \rightarrow 0$, the pointwise limits are

$$\lim_{a \rightarrow 0} B(x; a) = B_1 + (B_2 - B_1)H(x), \quad (\text{C.2})$$

where $H(x)$ is the Heaviside step function with $H(0) = 1/2$. On differentiating (C.1),

$$B'(x; a) = \frac{(B_2 - B_1)}{4a \cosh^2(x/2a)}. \quad (\text{C.3})$$

It will be shown here that *the sequence $B'(x; 1/n)$ defines the generalised function $(B_2 - B_1)\delta(x)$ where*

$$\int_{-\infty}^{\infty} \delta(x)F(x) dx = F(0), \quad (\text{C.4})$$

for any good function $F(x)$ in the sense of [9]. The small parameter a has been replaced by $1/n$ and following [9] :

$$\left| \int_{-\infty}^{\infty} B'(x; 1/n)F(x) dx - F(0) \right|$$

$$\begin{aligned}
&= \left| \int_{-\infty}^{\infty} \frac{n}{4} \operatorname{sech}^2 \frac{nx}{2} F(x) dx - F(0) \right| \\
&= \left| \int_{-\infty}^{\infty} \frac{n}{4} \operatorname{sech}^2 \frac{nx}{2} \{F(x) - F(0)\} dx \right| \\
&\leq \max |F'(\xi)| \int_{-\infty}^{\infty} \frac{n|x|}{4} \operatorname{sech}^2 \frac{nx}{2} dx, \quad -\infty < \xi < \infty \quad (\text{C.5})
\end{aligned}$$

where the last step is accomplished by recourse to the mean value theorem of the differential calculus.

It remains to be shown that the value of the integral in (C.5) tends to zero as $n \rightarrow \infty$. this is done by writing

$$\begin{aligned}
&\int_{-\infty}^{\infty} \frac{n|x|}{4} \operatorname{sech}^2 \frac{nx}{2} dx \\
&= \frac{n}{2} \int_0^{\infty} x \operatorname{sech}^2 \frac{nx}{2} dx \\
&= \frac{1}{2n} \int_0^{\infty} t \operatorname{sech}^2 \frac{t}{2} dt \\
&\rightarrow 0 \text{ as } n \rightarrow \infty.
\end{aligned}$$

It follows that

$$B'(x; 1/n) \sim (B_2 - B_1)\delta(x)$$

and, by the consistency properties proved in [9] page 18,

$$B''(x; 1/n) \sim (B_2 - B_1)\delta'(x).$$